CHAPTER 3 : STRUCTURAL PROPERTIES - RESULTS AND DISCUSSION

3.1 Thin Film Preparation

Eight batches of samples were deposited onto clear glass substrates via electron-beam evaporation technique. The sample preparation technique was discussed in chapter 2. The time of evaporation was changed as it produced films with different thickness. The films have shiny and smooth surfaces and all films showed good adherence to the substrate. The films were dark gray in colour and non-transparent to the visible eye. These films were later subjected to the techniques described in chapter 2 to determine their physical and electronic properties. The samples/films were prepared under the conditions mentioned in table 3.1.

Table 3.1 : Preparation conditions of CdTe thin films via e-beam evaporation technique.

Time of evaporation	30-120 s
High tension voltage	0.1 kV
Low tension current	20 mA
Substrate temperature	30 °C
Chamber pressure	1 x 10^{-5} torr

3.2 X-Ray Diffraction

All the samples (8 samples in each batch) showed polycrystalline phase with the presence of one or more peak corresponding to the CdTe. For the purpose of this report, samples which show clear variation in the thickness was chosen. A typical X-ray diffractogram of CdTe thin film is shown in figure 3.1. Diffraction peaks are observed at 2θ equals to 23.915 ° and 39.490° correspond, respectively to [111] and

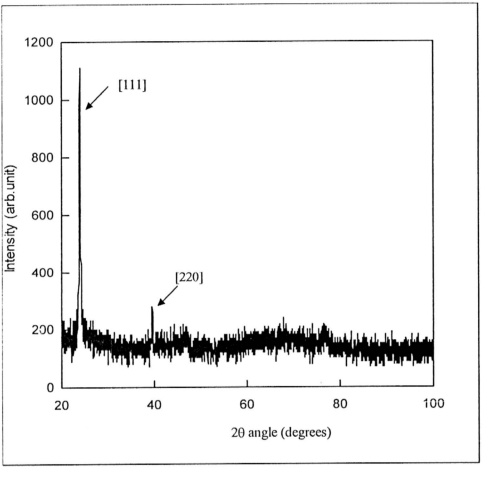

Figure 3.1 : Typical X-ray diffractogram of CdTe thin film deposited by e-beam evaporation technique.
Peaks at $2\theta = 23.915^{\circ}$ and 39.470° correspond to planes [111] and [220] respectively [44].

(220) planes of cubic (zinc blende) CdTe as confirmed by ASTM X-ray Powder File Data (Card 15-770).

In all samples the intensity of (220) plane peak was low or none in comparison with (111) plane peak in accordance with the results of Buch and Valentonic [58]. This indicate a preferential orientation of the nanocrystallites with (111) direction perpendicular to the substrate. Similar orientation of the CdTe zinc blende structure had been observed in CdTe films prepared by various techniques such as vacuum evaporation [43,59,60], r.f.sputtering [41], electron-beam evaporation [61] and hot wall flash evaporation [42].

The main features of the diffraction pattern are similar for all samples except the varying peak intensities. Figure 3.2 shows the X-ray diffractogram of the CdTe of thickness ranging from 500 - 1100 nm. As can be seen from the figure, the intensity of the peaks, of planes (111) and (220) increase with increasing film thickness due to the growth of the material incorporated in the diffraction process. It is also clear from the figure 3.2 that the degree of preferential orientation (111) to (220) increases with film thickness. This point can be shown as the variation in the intensity ratio of $I_{(111)}/I_{(220)}$, as illustrated in figure 3.3.

In the figure, it is clearly shown that the preferential orientation of growth (111), increases with film thickness. Preferential orientation growth of (111) to (220) is greater for films with thickness, $t > 600$ nm than for films with $t < 600$ nm. It explains the reason behind the structural data obtained where only (111) plane can be

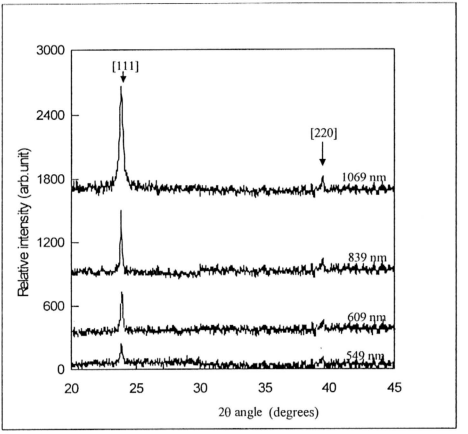

Figure 3.2 : X-ray diffractograms of CdTe thin films with different thickness.
Intensity of [111] and [220] plane peaks increases with film thickness
Film thickness is specified at the end of the diffractogram.

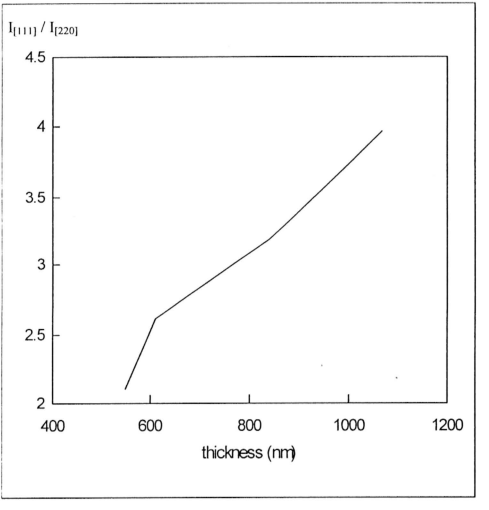

Figure 3.3 : Effect of film thickness on the degree of preferred orientation

seen in most of the samples prepared in this analysis as their thickness is in the range of 500-700 nm.

The lattice spacing and the respective planes of reflection [hkl] values were used to calculate the lattice constant of zinc blende CdTe thin films using the formula

$$\text{Lattice constant, } a = d\,(h^2 + k^2 + l^2)^{1/2}, \quad \ldots\ldots\ldots (3.1)$$

where d is the lattice spacing for single crystal CdTe in [111] direction [44]. The values are tabulated in table 3.2. Lattice constants that were obtained for the CdTe thin films are in the range of 6.384 Å - 6.542 Å. The average value of the calculated lattice constant is equal to 6.445 ± 0.037 Å, in agreement with the data estimated by El-Kadry [59] and Dharmadhikari [62]. This value is less compared to the single crystal lattice constant value of 6.481 Å [4,63]. The deviation of lattice constant from the single crystal lattice constant value is attributed to the changes in the stoichiometry of samples or sources or to the internal strain generated in the film during deposition as reported in reference 4.

Histogram in the figure 3.4 below illustrates the deviation of lattice constant of cubic CdTe thin films from the single crystal lattice constant value, 6.481 Å [4,63].

Almost 78 % of the samples showed negative relative difference in lattice constant while the remaining 22 % showed positive Δa. Negative difference can be attributed to compression/contraction in samples while positive difference to relaxation in materials. It has been reported that the films deposited via sputtering were found in a state of compressive stress in contrast to films deposited via vacuum evaporation [64].

Table 3.2 : Lattice parameters of CdTe thin films

sample	A/P	angle (deg)	plane	$d_{(111)}$ (Å)	a (Å)
b21771ct	p	23.915	111	3.7179	6.440
b21772ct	p	24.060	111	3.6958	6.401
b21773ct	p	24.115	111	3.6875	6.387
b21774ct	p	23.860	111	3.7264	6.454
b21775ct	p	23.960	111	3.7110	6.428
b21776ct	p	23.705	111	3.7504	6.496
b21777ct	p	24.125	111	3.6860	6.384
b21778ct	p	24.020	111	3.7019	6.412
b3861ct	p	23.960	111	3.7110	6.428
b3862ct	p	23.855	111	3.7271	6.456
b3863ct	p	23.960	111	3.7110	6.428
b3684ct	p	23.670	111	3.7558	6.505
b3685ct	p	23.745	111	3.7441	6.485
b3686ct	p	23.535	111	3.7771	6.542
b3687ct	p	23.830	111	3.7310	6.462
b3688ct	p	23.710	111	3.7496	6.494
b41381ct	p	23.930	111	3.7156	6.436
b41382ct	p	23.820	111	3.7325	6.465
b41383ct	p	23.875	111	3.7241	6.450
b41384ct	p	23.870	111	3.7248	6.452
b41385ct	p	23.735	111	3.7457	6.488
b41386ct	p	23.965	111	3.7103	6.426
b41387ct	p	23.935	111	3.7149	6.440
b41388ct	p	23.910	111	3.7187	6.441
b62591ct	p	24.010	111	3.7034	6.414
b62592ct	p	23.925	111	3.7164	6.437
b62593ct	p	23.665	111	3.7566	6.507
b62594ct	p	24.055	111	3.6966	6.403
b62595ct	p	23.920	111	3.7172	6.438
b62596ct	p	24.045	111	3.6981	6.405
b62597ct	p	24.065	111	3.6951	6.400
b62598ct	p	23.955	111	3.7118	6.429

{ Λ = amorphous ; P = Polycrystalline ; d = lattice spacing ; a = lattice constant)

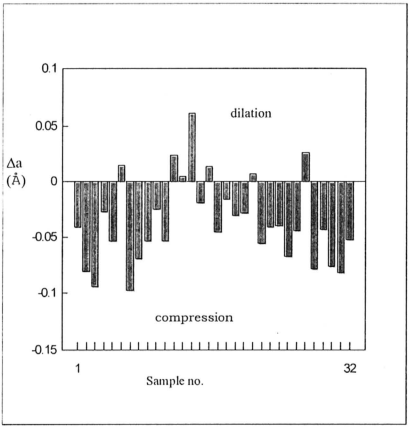

Figure 3.4 : Histogram showing the relative difference of lattice constant, Δa.
($\Delta a = a_o - a_s$; where $a_o = 6.481$ Å while a_s = lattice constant of the sample)

Negative difference in Δa as seen in the majority of the samples prepared under similar conditions, been interpreted as being the result of stress acting upon the CdTe lattice. The magnitude of stress has been estimated.

Since the crystallite composing the films exhibit preferential orientation, the estimation developed by Jimenez-Sandoval et.al. [41] were employed to calculate the magnitude of stress. By considering a cubic CdTe upon which a compressive stress S acts producing a strain *e*, given by

$$e = (d_o - d) / d_o \qquad \text{..... (3.2)}$$

where the lattice parameters are measured along the [111] direction before (d_o) and after (d) the stress is applied.

Stress and strain components are related through the elastic compliance tensor whose nonzero components for cubic crystal are S_{11}, S_{12} and S_{44} [65]. By using the elastic compliance constants given by A.Gavini [66] for S_{11} and S_{12} for CdTe as 4.27 x 10^{-12} cm^2/dyn and -1.73 x 10^{-12} cm^2/dyn respectively, the applied stress, S along the [111] direction of a cubic crystal was calculated as

$$S = e / (S_{11} + 2S_{12}) . \qquad \text{..... (3.3)}$$

The values are tabulated in table 3.3.

Tabulated value of stress shows the increase with decreasing lattice spacing or indirectly with the decreasing lattice constant. The origin of stress that contributes to this strain in samples has been reviewed in many papers. According to T.J.Vink [67], at relatively low pressure of deposition, the arriving atoms have a high kinetic energy and the resulting film develop a dense microstructure and experiences compressive stress.

Table 3.3 : Lattice spacing, strain, stress and cluster size

sample	d(111) (Å)	Δd (Å)	Strain, *e* (Å/Å)	Stress, S (cm^2/dyn)	D_x (nm)
b21771ct	3.7179	0.0241	0.00644	7.95×10^9	33.88
b21772ct	3.6958	0.0462	0.0123	1.52×10^{10}	81.33
b21773ct	3.6875	0.0545	0.0145	1.80×10^{10}	101.67
b21774ct	3.7264	0.0156	0.00416	5.14×10^9	40.65
b21775ct	3.711	0.031	0.00828	1.02×10^{10}	67.76
b21776ct	3.7504	-0.00839	-0.00224	-2.77×10^9	81.27
b21777ct	3.686	0.0560	0.0149	1.85×10^{10}	40.67
b21778ct	3.7019	0.0401	0.0107	1.32×10^{10}	81.32
b3861ct	3.711	0.031	0.00828	1.02×10^{10}	58.08
b3862ct	3.7271	0.0149	0.00398	4.91×10^9	40.65
b3863ct	3.711	0.031	0.00828	1.02×10^{10}	58.08
b3684ct	3.7558	-0.0138	-0.00368	-4.55×10^9	50.79
b3685ct	3.7441	-0.00209	-0.000561	-6.92×10^8	81.3
b3686ct	3.7771	-0.0351	-0.00938	-1.16×10^{10}	67.71
b3687ct	3.731	0.011	0.00293	3.63×10^9	50.81
b3688ct	3.7496	-0.00759	-0.00203	-2.51×10^9	45.15
b41381ct	3.7156	0.0264	0.00705	8.71×10^9	36.69
b41382ct	3.7325	0.00949	0.00253	3.13×10^9	45.16
b41383ct	3.7241	0.0179	0.00478	5.91×10^9	67.75
b41384ct	3.7248	0.0172	0.00459	5.67×10^9	101.62
b41385ct	3.7457	-0.00369	-0.000988	-1.22×10^9	81.28
b41386ct	3.7103	0.0317	0.00847	1.05×10^{10}	67.76
b41387ct	3.7149	0.0271	0.00724	8.94×10^9	45.17
b41388ct	3.7187	0.0233	0.00622	7.67×10^9	36.69
b62591ct	3.7034	0.0386	0.0103	1.27×10^{10}	50.82
b62592ct	3.7164	0.0256	0.00684	8.45×10^9	40.65
b62593ct	3.7566	-0.0145	-0.00390	-4.81×10^9	50.79
b62594ct	3.6966	0.0454	0.0121	1.50×10^{10}	50.82
b62595ct	3.7172	0.0248	0.00662	8.19×10^9	45.17
b62596ct	3.6981	0.0439	0.0117	1.45×10^{10}	50.83
b62597ct	3.6951	0.0469	0.0125	1.55×10^{10}	50.83
b62598ct	3.7118	0.0302	0.00807	9.96×10^9	36.96

($\Delta d = d_o - d$; where $d_o = 3.742$ Å [44] ; D_{XRD} = average cluster size)

The compressive stress is caused by atomic peening which is caused by the impact of energetic particles (reflected neutrals/sputtered atoms) [68,69]. During sputtering, the sputtered atoms are ejected with energies of the order of 10 eV, about 100 times the energy of evaporated atoms [64]. These atoms bombarded the surface films which is judiciously named as 'peening' of atoms [69]. Peening causes atoms to be incorporated in the growing film with a density higher than would be obtained otherwise since with sufficient energy atoms may be forced into spaces too small to accommodate them under thermal equilibrium conditions, thus leads to compressive stresses in films.

Stresses in the film also appear due to the large thermal expansion coefficient of CdTe with respect to that of the clear glass substrates [41].

22% of the samples deposited show the presence of tensile stress leading to expansion in the lattice spacing and constants. Expansion in lattice spacing is usually related to the stoichiometry of the sample. It is reported that CdTe grown from Te-rich CdTe showed larger lattice constant compared to single crystal value [4]. In the present analysis as confirmed by the EDX results, all samples have rich tellurium content compared to cadmium (3:2). Thus the behaviour in the expansion caused can be explained only in terms of the presence of voids in the sample. Presence of voids or gaps introduce tensile stresses which causes expansion of lattice constant and lattice spacing. Deposition at higher pressure also results in films exhibiting an open porous microstructure, producing tensile stress.

All samples produce appreciable diffraction broadening and it is assumed that this arises from small crystallites and internal stresses [70]. According to Langford and Wilson [71], the maxima of the diffraction pattern are broadened by an amount inversely proportional to the crystallite size, that the broadening in radians at full width half maximum (FWHM) was used to calculate the average crystallite size, D_{XRD}, using the Scherrer formula,

$$D_{XRD} = k\lambda / (\beta \cos \theta), \qquad \text{..... (3.4)}$$

where k = Scherrer constant

β = pure broadening due to the size of the crystal

θ = Bragg angle (in radians)

λ = wavelength of the radiation.

The broadening obtained in this procedure was corrected for instrumental broadening by [72]

$$B^2 = \beta^2 + b^2, \qquad \text{..... (3.5)}$$

where B is the broadening from the diffractogram and b is the broadening due to instrument. It must be strongly emphasized that the relative rather than the absolute size is obtained.

The crystallite sizes were calculated by assuming the instrumental broadening of 0.15° and Scherrer constant of 0.8551 for cubic crystals [62] at a reflection plane of [111]. The crystallite are usually irregular in shape but on average they may often be regarded as having regular external form. As for that the crystallite sizes obtained from [111] reflection is often referred to as apparent crystal size or

average crystallite size normal to the reflecting plane [71]. The calculated crystallite sizes are shown in table 3.3. The crystallite sizes vary with film thickness as illustrated in figure 3.5. The cluster sizes increases linearly with film thickness of CdTe. The crystallite sizes of CdTe becomes larger in the thicker films. As the measured crystallite size is normal to the (111) plane direction, the observed increase in the crystallite size may be interpreted in terms of a columnar grain growth. Similar observations were reported for II-VI semiconductor compounds prepared by various techniques[8,54,73,74].

The crystallite sizes obtained via e-beam evaporation technique shows a distribution as shown in the histogram in figure 3.6. The crystallite sizes vary in from 30nm to 110 nm. The mean crystallite size obtained is 47.17 nm. Majority of the crystallites obtained (52.5 %) were in the range of size 30-40 nm. So, it can be concluded here that the e-beam evaporation technique employed in this study under the conditions verified earlier can yield nanocrystallites with 52.5% crystallites in the range of 30-40 nm.

Diffractograms of CdTe thin films with varying cluster sizes showed a variation in the breadth of the peak (or in its full width at half maximum of the peak) as shown in the figure 3.7. The peaks of reflecting plane (111) becomes narrower (FWHM reduces) as the cluster size increases.

Moreover a slight shift in the position (2θ value) of the peak is seen, which is related to the shift in lattice spacing. This is further related to the deviation in the lattice constant as shown in figure 3.8. The lattice constant increases with decreasing

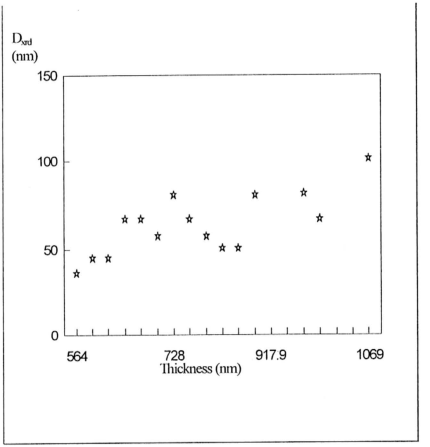

Figure 3.5: Dependence of cluster size on the thickness of CdTe films

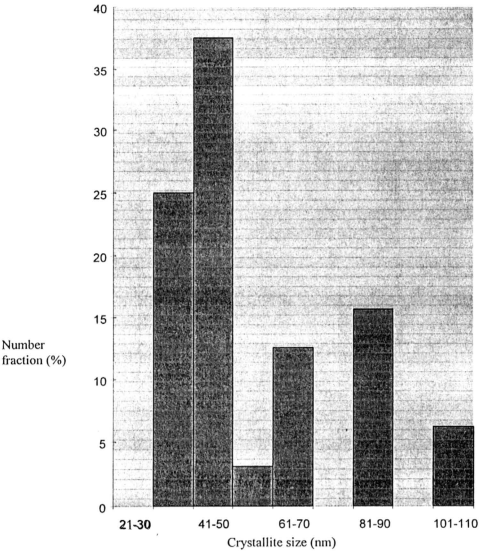

Figure 3.6: Histogram showing the distribution of nanocrystallites in CdTe thin films.

(52.5 % of the crystallites are of the size range 30-50 nm ; mean crystallite size obtained is 47.17 nm; The samples are prepared for 30s evaporation)

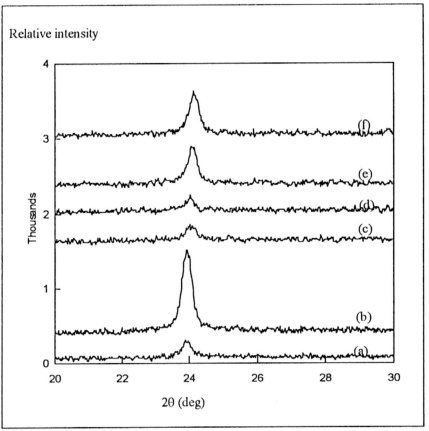

Figure 3.7 : Diffractograms of CdTe with varying crystallite sizes.
[(a) - D_x = 33.88 nm ; FWHM = 0.240 °
(b)- D_x = 40.65 nm ; FWHM = 0.200 °
(c)- D_x = 67.76 nm ; FWHM = 0.120 °
(d)-D_x = 81.32 nm ; FWHM = 0.100 °
(e)- D_x = 81.33 nm ; FWHM = 0.100 °
(f)- D_x = 101.67 nm ; FWHM = 0.080 ° , D_x = crystallite size and FWHM = full width at half maximum peak]

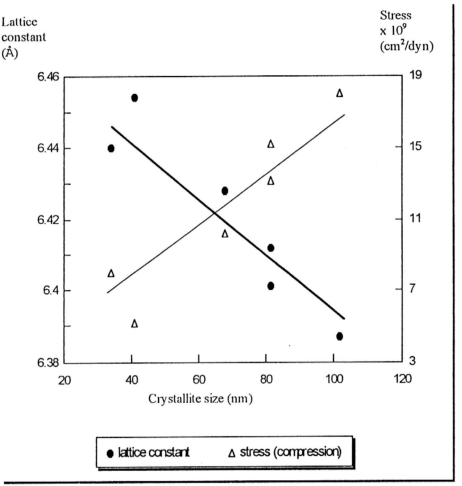

Figure 3.8 : Variation of lattice constant and stress with cluster size.
Lattice constant approaches the single crystal value as the crystallite size decreases. This is accompanied by the reduction in the compression in the crystallites.

crystallite size. The increase in the lattice constant is observed to occur towards the single crystal lattice constant value (6.482 Å) as the crystallite size decreases. In the diagram , also illustrated is the variation of the stress (compression) with cluster size to explain the changes observed in the dilation of lattice constant. The compression is reduced as the crystallite size becomes smaller, which can be interpreted as the relaxation of atoms in the crystallite to attain the single crystal orientation.

3.3 SEM, TEM and EDAX

CdTe samples for SEM, TEM and EDAX analysis were prepared separately under similar conditions described in table 3.1, due to instrumental limitations. Samples for SEM and EDAX analysis were coated onto glass substrates with dimensions of 4 mm x 4 mm, while for TEM analysis the samples were prepared by coating CdTe directly onto copper grids with mesh count of 300.

Scanning electron micrographs of CdTe samples are shown in figures 3.8 (a) to 3.8 (f). All photographs show polycrystalline surfaces of CdTe thin films. Photographs at lower magnification display large grains embedded in matrix of finer grains while those at higher magnification showed fine polycrystalline phase. The grain sizes varied from 100 to 400 nm. This size is large compared to the average crystallite size that was estimated from XRD spectra, eventhough these samples were prepared along with XRD samples under same conditions, in accordance with the report by A.A.Ramadan et. Al.[75] , that the grains usually gives larger size (from SEM) than those determined by X-ray broadening. This is because the coherent diffraction domains are smaller than the average size according to direct observation.

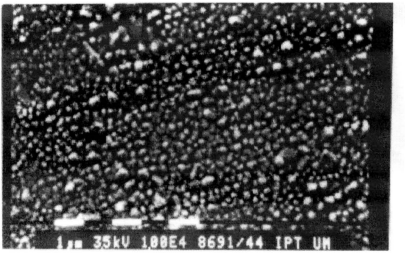

Figure 3.8 (a) : Scanning electron micrograph of CdTe

(sample b21772ct) at 10 000 X

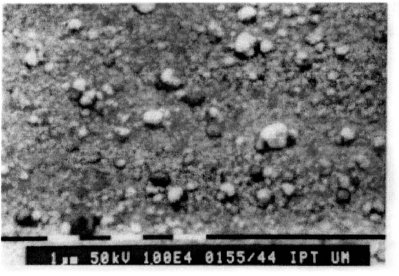

Figure 3.8 (b) : Scanning electron micrograph of CdTe thin film

(ample cad-1) at 10 000 X

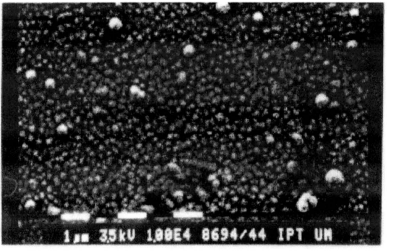

Figure 3.8 (c) : Scanning electron micrograph of CdTe thin film (sample CAD-2) at 10 000 X

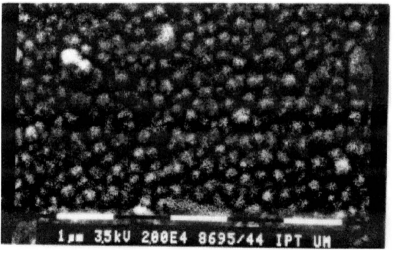

Figure 3.8 (d) : Scanning electron micrograph of CdTe thin film (sample CAD-2) at 20 000 X

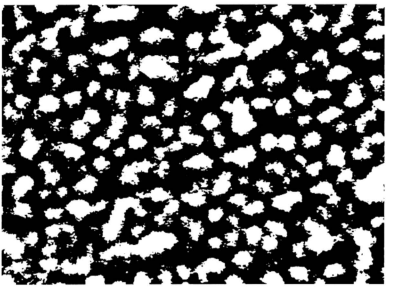

Figure 3.8 (e) : SEM photograph of CdTe thin film (sample CAD-3) at 100 000 X
(Clear distribution of clusters can be observed at this magnification. However, the grain boundary is not very clear as the resolution becomes weak at this magnification)

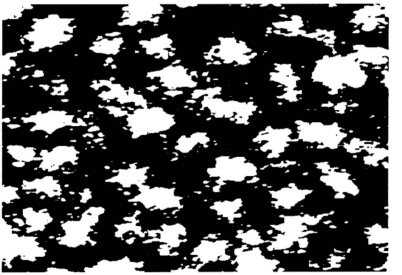

Figure 3.8 (f) : SEM photograph of CAD-3 at 150 000 X

Also reported that some grain boundaries, such as low-angle boundaries may be missed in direct observation. Therefore, the values of the crystallite size determined by XRD are more valuable in correlation with the physical properties. In the photographs, the white and dark spots represent tellurium(non-conducting) and cadmium (conducting) respectively. In the present approach of estimation, the dark area that separates the white grains was taken as the mere boundary of the grains. It is believed that there is a possibility of the existence of a thin layer of tellurium, overlaying these grains which accounts for larger grain estimation. It is believed also that the grains observed are clusters of small crystallites. The instrumental limitation does not allow further resolving of these grains into crystallites. From the results of XRD and SEM, it is estimated each and every grains observed in SEM photographs might represent clustering of 3-10 nanocrystallites (with average size of 47 nm).

There is a distribution of grain size observed in the SEM photographs. The distribution is skewed towards small grain size as seconded by the crystallite size distribution shown in figure 3.6, earlier. The variation in the grains sizes is an indication of nonuniformity in the crystallization during deposition and also account for non uniformity in thickness of the film. This idea was used to explain the behaviour of CdTe in optical and electronic properties.

TEM photographs show similar morphology of CdTe thin films. Since the films were prepared onto copper grids, no complete crystalline phase was observed. The films were estimated of thickness less than 300 nm as films beyond this thickness cannot be investigated under TEM. The thin films are of amorphous in nature with a

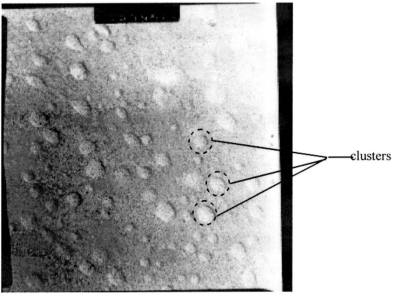

Figure 3.9 (a) : TEM micrograph of CdTe

(at 22 000 X magnification, shows the distibution of clusters in the thin film)

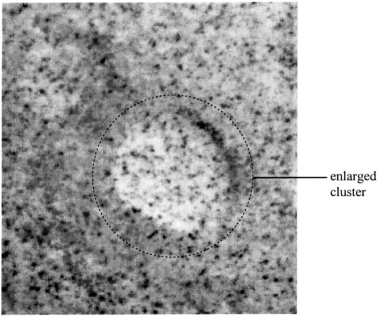

Figure 3.9 (b) : TEM Micrograph of CdTe thin film

(at 56 000X magnification; shown is the elarged cluster region)

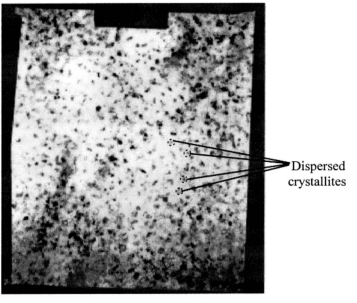

Figure 3.9 (c) : TEM micrograph of CdTe thin film

(at 80 000 X magnification showing the interior section of a cluster)

small number of grains immersed in the amorphous media as shown in figures 3.9 (a) and (b). The magnification of this grain is shown in figure 3.9 (c). It indicates the presents of nanocrystallites as suspected in the SEM photographs earlier. These crystallites are of sizes 5-15 nm. The invariably small crystallite sizes observed can be reasoned by the thin film thickness. As discussed before the average crystallite size increases with film thickness (figure 3.5), so the obtained grain size is rather a predicted result. This confirms that small nanocrystallites agglomerate to form grains that are clearly seen in both SEM and TEM photographs. XRD being the only technique which enables the estimation of average grain size directly. However this technique gives no information regarding the distribution of nanocrystallites in the films, where this information is vital in device fabrication using nanocrystallites [76]. It has been reported that TEM micrograph analysis coupled with morphological filtering using computer yield a better estimation of crystallite sizes and distribution [77-79].

Energy dispersive analysis by X-ray (EDAX) revealed that the films contain Cadmium and Tellurium as the major constituents. In the initial scanning elements such as potassium, sodium, magnesium, calcium, aluminium, silicon besides Cadmium and Tellurium were observed. By setting the baseline level closer to 0.01 ppm, these elements were removed from the spectra.. A typical spectrum of EDX analysis is shown in figure 3.10. The intensity of the peaks varied with cadmium and tellurium content. The details are tabulated in table 3.4.

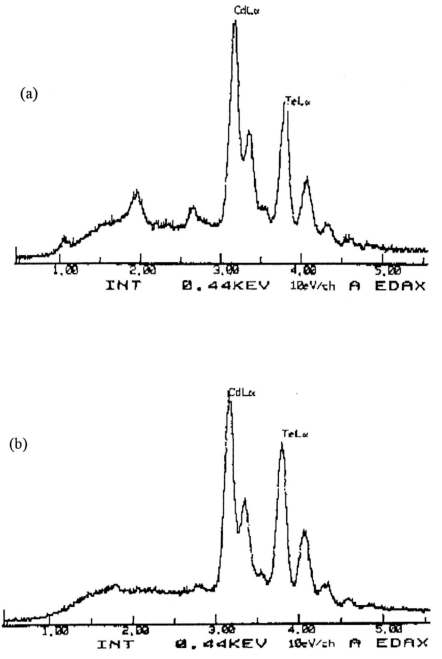

Figure 3.10 : Typical EDX spectra for CdTe thin films

[(a)- sample CAD-1 and (b)- sample CAD-3]

In order to obtain the stoichiometry of the deposited thin films, the ratio of cadmium to tellurium were calculated. It is clear from table 3.4 that all the samples showed high content of tellurium. On this basis it is concluded that the entire set of

Table 3.4 : Microprobe analysis results of CdTe thin films

Sample	% of Cadmium	% of Tellurium	Ratio of Cd : Te	Thickness, t (nm)
CAD-1	37.63	62.37	1 : 1.66	1004.2
CAD-2	36.97	63.03	1 : 1.71	764.1
CAD-3	37.59	62.41	1 : 1.66	1014.6
CAD-4	39.28	60.72	1 : 1.55	584.5
CAD-5	37.78	62.22	1 : 1.65	1061.1
CAD-6	36.78	63.22	1 : 1.72	821.1

(The thickness of the films was calculated as an average value of the films' thickness obtained in a particular batch)

films deposited and analyzed in this work are of tellurium rich CdTe thin films. Tellurium was present in an approximate ratio 1.5:1 to cadmium. Approximately the ratio can be said as 3:2 for Te:Cd. CdTe when heated dissociates into Cd and Te_2 according to [80]

$$CdTe_{(s)} \longrightarrow Cd_{(g)} + 1/2\ Te_{2\ (g)}$$

Changes in the vapour composition of Cd/Te_2 is believed to cause the presence of excess tellurium in the thin films. Moreover high sticking coefficient of tellurium compared to cadmium [8] might also account for high tellurium content in the deposited films. Similar ratio as tabulated in table 3.4 is also seen for white spot, dark spot and broad scan analysis of the samples shown in figure 3.8. This indicates that

tellurium is well distributed in the films. As there was no peak in the XRD spectra indicative of tellurium alone, it can be proposed that the presence of excess tellurium could account for high stresses in the films due to interstitial introduction of Te atoms in Cd-Te lattice. It is also to be noted that the stoichiometry of the films (CAD-1 to CAD-6) was found to be invaried with film thickness.